



OPEN ACCESS

EDITED BY

Chung Hoow Kok,
University of Adelaide, Australia

REVIEWED BY

Ahmet Emre Eskazan,
Istanbul University-Cerrahpasa, Türkiye
Jignesh D. Dalal,
Case Western Reserve University,
United States
Mario Tiribelli,
University of Udine, Italy

*CORRESPONDENCE

Ingolf Cascorbi

✉ cascorbi@pharmakologie.uni-kiel.de

RECEIVED 05 April 2023

ACCEPTED 24 May 2023

PUBLISHED 13 June 2023

CITATION

Kaehler M, Osteresch P, Künstner A, Vieth SJ, Esser D, Möller M, Busch H, Vater I, Spielmann M, Cascorbi I and Nagel I (2023) Clonal evolution in tyrosine kinase inhibitor-resistance: lessons from *in vitro*-models. *Front. Oncol.* 13:1200897. doi: 10.3389/fonc.2023.1200897

COPYRIGHT

© 2023 Kaehler, Osteresch, Künstner, Vieth, Esser, Möller, Busch, Vater, Spielmann, Cascorbi and Nagel. This is an open-access article distributed under the terms of the [Creative Commons Attribution License \(CC BY\)](https://creativecommons.org/licenses/by/4.0/). The use, distribution or reproduction in other forums is permitted, provided the original author(s) and the copyright owner(s) are credited and that the original publication in this journal is cited, in accordance with accepted academic practice. No use, distribution or reproduction is permitted which does not comply with these terms.

Clonal evolution in tyrosine kinase inhibitor-resistance: lessons from *in vitro*-models

Meike Kaehler¹, Pia Osteresch¹, Axel Künstner^{2,3}, Stella Juliane Vieth¹, Daniela Esser⁴, Marius Möller^{2,3}, Hauke Busch^{2,3}, Inga Vater⁵, Malte Spielmann^{5,6}, Ingolf Cascorbi^{1*} and Inga Nagel^{1,5}

¹Institute of Experimental and Clinical Pharmacology, University Hospital Schleswig-Holstein, Campus Kiel, Kiel, Germany, ²Medical Systems Biology Group, University of Lübeck, Lübeck, Germany, ³Institute of Cardiogenetics, University of Lübeck, Lübeck, Germany, ⁴Institute of Clinical Chemistry, University Hospital Schleswig-Holstein, Kiel, Germany, ⁵Institute of Human Genetics, University Hospital Schleswig-Holstein, Kiel, Germany, ⁶Institute of Human Genetics, University Hospital Schleswig-Holstein, Lübeck, Germany

Introduction: Resistance in anti-cancer treatment is a result of clonal evolution and clonal selection. In chronic myeloid leukemia (CML), the hematopoietic neoplasm is predominantly caused by the formation of the BCR::ABL1 kinase. Evidently, treatment with tyrosine kinase inhibitors (TKIs) is tremendously successful. It has become the role model of targeted therapy. However, therapy resistance to TKIs leads to loss of molecular remission in about 25% of CML patients being partially due to BCR::ABL1 kinase mutations, while for the remaining cases, various other mechanisms are discussed.

Methods: Here, we established an *in vitro*-TKI resistance model against the TKIs imatinib and nilotinib and performed exome sequencing.

Results: In this model, acquired sequence variants in *NRAS*, *KRAS*, *PTPN11*, and *PDGFRB* were identified in TKI resistance. The well-known pathogenic *NRAS* p.(Gln61Lys) variant provided a strong benefit for CML cells under TKI exposure visible by increased cell number (6.2-fold, $p < 0.001$) and decreased apoptosis (-25%, $p < 0.001$), proving the functionality of our approach. The transfection of *PTPN11* p.(Tyr279Cys) led to increased cell number (1.7-fold, $p = 0.03$) and proliferation (2.0-fold, $p < 0.001$) under imatinib treatment.

Discussion: Our data demonstrate that our *in vitro*-model can be used to study the effect of specific variants on TKI resistance and to identify new driver mutations and genes playing a role in TKI resistance. The established pipeline can be used to study candidates acquired in TKI-resistant patients, thereby providing new options for the development of new therapy strategies to overcome resistance.

KEYWORDS

chronic myeloid leukemia, drug resistance, imatinib, nilotinib, *PTPN11*, *PDGFRB*, *NRAS*, *KRAS*

1 Introduction

Despite tremendous advances within the last decades, therapy failure is still a significant burden in anti-cancer therapy. Tumor cells tend to escape chemotherapy by clonal evolution and selection of resistant subclones, resulting in a relapse in therapy. Next-generation sequencing aims to find promising candidate variants in resistant cancer cell sublines. Such approach may further be helpful for molecular tumor boards to adapt the targeted therapy regimen for each patient (1).

The myeloproliferative syndrome chronic myeloid leukemia (CML) became a role model for effective and successful targeted therapy. CML is a rare neoplasm, mainly caused by reciprocal translocation t(9;22)(q34;q11), resulting in the formation of the *BCR::ABL1* fusion gene (2). In many cases, it is successfully treated using tyrosine kinase inhibitors (TKIs), especially the 2-phenylaminopyrimidine imatinib, which binds to the *BCR::ABL1* kinase and, thereby, prevents phosphorylation of downstream targets (3). Although overall 10-year survival rates are high at 83%, 20 to 25% of all patients suffer from therapy failure within five years of treatment (4, 5). Second and third-generation TKIs, namely nilotinib, dasatinib, bosutinib, and ponatinib, were developed to overcome such resistances with variable success (6, 7). TKI resistance occurs either dependent or independent from *BCR::ABL1* kinase alterations. The first-mentioned is predominantly caused by mutations in *BCR::ABL1* (e.g., *ABL1* p.(Tyr253His), p.(Glu255Val) or p.(Thr315Ile)) preventing binding of the TKIs to the kinase domain or by *BCR::ABL1* gene amplification and overexpression (8). For *BCR::ABL1*-independent resistance, several mechanisms are discussed, e.g., overexpression of drug efflux transporters, especially the ATP binding cassette (ABC) transporter family members p-glycoprotein (P-gp, ABCB1) or breast cancer resistance protein (BCRP, ABCG2), the adaptation of signaling pathways or deregulation of gene expression (9, 10). In addition, genetic aberrations, e.g., trisomy 8 or mutations affecting runt-related transcription factor 1 (*RUNX1*), were shown to contribute to the progression into blast crisis or selection of TKI-resistant clones in patients (11, 12).

Besides clinical studies, *in vitro*-models can be applied to study mechanisms of drug resistance in detail. Such models are pivotal tools as findings derived from these models were successfully translated into the clinic, e.g., to predict drug efficacy and improve treatment protocols (13). Drug resistance of a tumor cell line can be acquired *in vitro* by exposure to slowly increasing anticancer drug concentrations or by pulse treatment.

Here, we used exome sequencing to study genetic variants in a TKI resistance CML *in vitro*-model. For this purpose, we established biological replicates of imatinib and nilotinib resistance. We report on sequence variants evolving in imatinib and nilotinib resistance development. Further, we investigate the influence of the candidate variants *PTPN11* p.(Tyr279Cys), *PDGFRB* p.(Glu578Gln), and *NRAS* p.(Gln61Lys) on the response to TKI treatment.

2 Material and methods

2.1 Reagents, cell lines, and generation of resistant cells

If not indicated otherwise, chemicals and reagents were obtained from Sigma-Aldrich (Munich, Germany) or Carl Roth (Karlsruhe, Germany).

K-562 cells (RRID: CVCL_0004), established from the pleural effusion of a 53-year-old woman (14), were obtained from the German Collection of Microorganisms and Cell Cultures (DSMZ, Braunschweig, Germany). Cell maintenance, generation of biological replicates of TKI-resistant sublines, and analyses of cell line authenticity were described elsewhere (15, 16). Cells were resistant against lowIM (0.5 μ M imatinib), highIM (2 μ M imatinib), lowN (0.05 μ M nilotinib) and highN (0.1 μ M nilotinib). The concentrations were chosen to reflect the clinically typical range of estimated imatinib plasma concentration, as well as the 20-fold higher potency of nilotinib.

2.2 RNA and DNA extraction

Total RNA was isolated using E.Z.N.A Total RNA kit 1 (Omega bio-tek, Norcross, GA, USA). Cell line DNA was purified using Genra Puregene Kit (Qiagen, Hilden, Germany).

2.3 Exome sequencing

Exome sequencing was performed using Illumina InView Human Exome Advance sequencing technology, a random-primed cDNA library, 60x coverage, and 2 x 150 bp read length at Eurofins Genomics (Ebersberg, Germany). Raw data was mapped against GRCh38. Exome data was processed similarly to Künstner et al. (17). For the detailed bioinformatic analysis, see [supplement](#).

2.4 MiSeq

Exome sequencing data was validated using Next Generation Sequencing (NGS) SBS technology with Illumina MiSeq after PCR amplicon preparation with the Nextera XT Sequencing Kit (Illumina, San Diego USA). For this purpose, amplicons of the respective genes were generated using gene-specific primers, primer-specific annealing temperatures and MyTaq DNA Polymerase (Meridian Bioscience, Memphis, TN, USA). ([Supplementary Table 1](#)). Genomic DNA from 2 μ M imatinib resistant K-562 cells replicate 2, and 0.1 μ M nilotinib resistant K-562 cells replicate 2 served as templates. PCR products were extracted using GeneJet Gel Extraction Kit (Thermo Fisher Scientific, Darmstadt, Germany) according to the manufacturer's recommendations. MiSeq was performed according to the manufacturer's protocol, as already described (18).

2.5 Genome-wide expression analyses

Microarrays were performed using Clariom S Arrays (Affymetrix; Thermo Fisher Scientific) as previously described (16). Briefly, RNA was isolated using miRVANA microRNA isolation kit (Thermo Fisher), and 100 ng were hybridized onto the arrays according to the manufacturer's protocol. Further details about data processing and analysis are given in the supplement.

2.6 Whole-cell lysates and immunoblotting

Whole-cell lysates and immunoblotting were performed as described elsewhere (19, 20). Blots were probed with the following antibodies obtained from Santa Cruz or CST (Danvers, MA, USA): phospho-ERK: Cat# sc-7383, RRID AB_627545, 1:1000; ERK: Cat# sc-514302, RRID : AB_2571739, 1:1000; SHP2: Cat# 3397, RRID: AB_2174959, 1:1000; PDGFR β : Cat# sc-374573, RRID: AB_10990921, 1:100; pan-RAS: Cat# sc-166691, RRID: AB_2154229, 1: 200; GAPDH: Cat# sc-47724, RRID: AB_627678, 1:2000; anti-rabbit: Cat# 926-32211, RRID: AB_621843; Cat# 926-926-68071, RRID: AB_10956166; anti-mouse: Cat# 926-32210, RRID: AB_621842, Cat# 926-680707, RRID: AB_10956588; all 1:10,000, LiCOR (Bad Homburg, Germany). Primary antibodies were diluted in Intercept/TBS blocking solution (LiCOR) supplemented with 0.2% Tween-20, secondary antibodies were diluted in TBS supplemented with 0.1% Tween-20. Total protein staining was performed using Revert 700 Total Protein Stain Solution according to the manufacturer's protocol (LiCOR). Densitometry was performed using Empiria Studio 1.2 (LiCOR).

2.7 Inhibition assay

PTPN11 phosphatase activity was blocked using the allosteric inhibitor RMC-4550 (ProbeChem, Shanghai, China). For this purpose, 1×10^6 cells per sample were seeded onto 12 well plates and incubated with 1.5 μ M RMC-4450 for 3 h in a cell culture incubator. Subsequently, cells were collected, and immunoblotting was performed as described above.

2.8 Cloning

The coding regions of *PTPN11* (NM_002834.5) and *NRAS* (NM_002524.5) were amplified using cDNA from highIM-R2 and highN-R2 cells. *PDGFRB* coding plasmid was obtained from Sino Biological (NM_002609.3, HG10514-G, Eschborn, Germany). The amplicons were cloned into the pSelect-puromycin-mcs vector (Sigma-Aldrich) using the CloneAmp HiFi PCR premix (Takara) with gene-specific primers and primer-specific annealing temperatures (Supplementary Table S1) including the restriction enzymes BamHI and NcoI/NheI (NEB), cloning enhancer and the In-Fusion HD Kit (Takara). *PDGFRB* p.(Glu578Gln) was inserted using Q5 site-directed mutagenesis kit (NEB) using the primers *PDGFRB_Glu578Gln_F* and *PDGFRB_Glu578Gln_R* at 60°C

annealing temperature and 3 min elongation time according to the manufacturer's protocol (Supplementary Table S1). Sequence identity was confirmed using Sanger sequencing.

2.9 Transient and stable transfection

Transient transfection was performed using nucleofection and the nucleofector 2 b device (Lonza, Cologne, Germany). 2×10^6 cells were transfected with 5 or 10 μ g of the respective plasmid or empty vector control for plasmid transfection or 100 nM Ambion Silencer Select s11524 or negative control #1 for siRNA-mediated knockdown of *PTPN11*. 24 h after transfection, cells were seeded onto respective cell culture plates to analyze cellular fitness followed by 24-48 h exposure to 2 μ M imatinib or 100 nM nilotinib or used for expression analyses as described elsewhere. After incubation time, cells were subducted for subsequent cellular fitness assays as described below. Stably transfected cells were generated by selecting puromycin-resistant cells after 4 weeks of exposure to 1 μ g/ml puromycin (Invivogen, Toulouse, France).

2.10 Cellular fitness assays

Cellular fitness was analyzed as previously described (16, 18, 19). Briefly, cell numbers were obtained by trypan blue staining, WST-1 (Sigma-Aldrich), Caspase Glo 9 Assay (Promega), Bromodeoxyuridine proliferation assay (Merck, Darmstadt, Germany), and MKI ELISA Kit (MyBioSource, San Diego, CA, USA) according to the manufacturers' recommendations. Data was analyzed by normalizing TKI-treated to non-treated samples, followed by statistical analyses as described below. For analyses of total cell number, proliferation, and apoptosis during the development of imatinib resistance, 0.5×10^6 cells/ml were seeded into cell culture flasks and exposed to 0.1 μ M imatinib for 21 days. Cells were counted and cultivated dependent on the cell density. After 21 days, Ki-67 expression and caspase 9 activity were measured as described above. The analyses of 0.2 and 0.3 μ M imatinib were performed accordingly.

2.11 Statistical analysis

Unless not stated otherwise, statistical analysis was performed using one-way ANOVA, Dunnett's test and/or student's t-test and the GraphPad prism software (Version 8.0 for Windows, San Diego California, USA).

3 Results

3.1 Genetic analyses reveal large differences between biological replicates of imatinib and nilotinib resistance

To analyze clonal evolution in TKI resistance, imatinib and nilotinib-resistant sublines derived from TKI-sensitive K-562 cells were established by step-wise exposure to increasing TKI

concentrations (Figure 1A). Cell lines developing resistance against 0.5 μM imatinib (lowIM) or 2 μM imatinib (highIM), as well as 0.05 μM nilotinib (lowN) or 0.1 μM nilotinib (highN) were obtained generating four biological replicate cell lines of imatinib and two of nilotinib resistance (Figure 1B). Subsequently, genetic variants in these twelve TKI-resistant sublines were analyzed by exome sequencing and compared to TKI-sensitive K-562 cells.

First, non-intronic single nucleotide variants (SNVs) exclusively present in TKI-resistant cells were identified by excluding SNVs present in TKI-sensitive K-562 (VAF < 0.05) and applying a ΔVAF

> 15% in the TKI-resistant sublines compared to TKI-sensitive cells. The number of variants differed between 103 and 195 in the TKI-resistant sublines (Figure 1C, Supplementary Table S2). For IM-R1 and IM-R4, the majority of SNVs, 128 and 60, respectively, were newly acquired in highIM, whereas for IM-R2 and IM-R3, as well as in N-R1 and N-R2, the majority of SNVs were already present in the respective lowIM or lowN sublines (IM-R2: 61, IM-R3: 87, N-R1: 76, N-R2: 51, Figure 1C). The total number of SNVs differed between the biological replicates of TKI resistance but increased compared to TKI-sensitive cells in all TKI-resistant cell lines

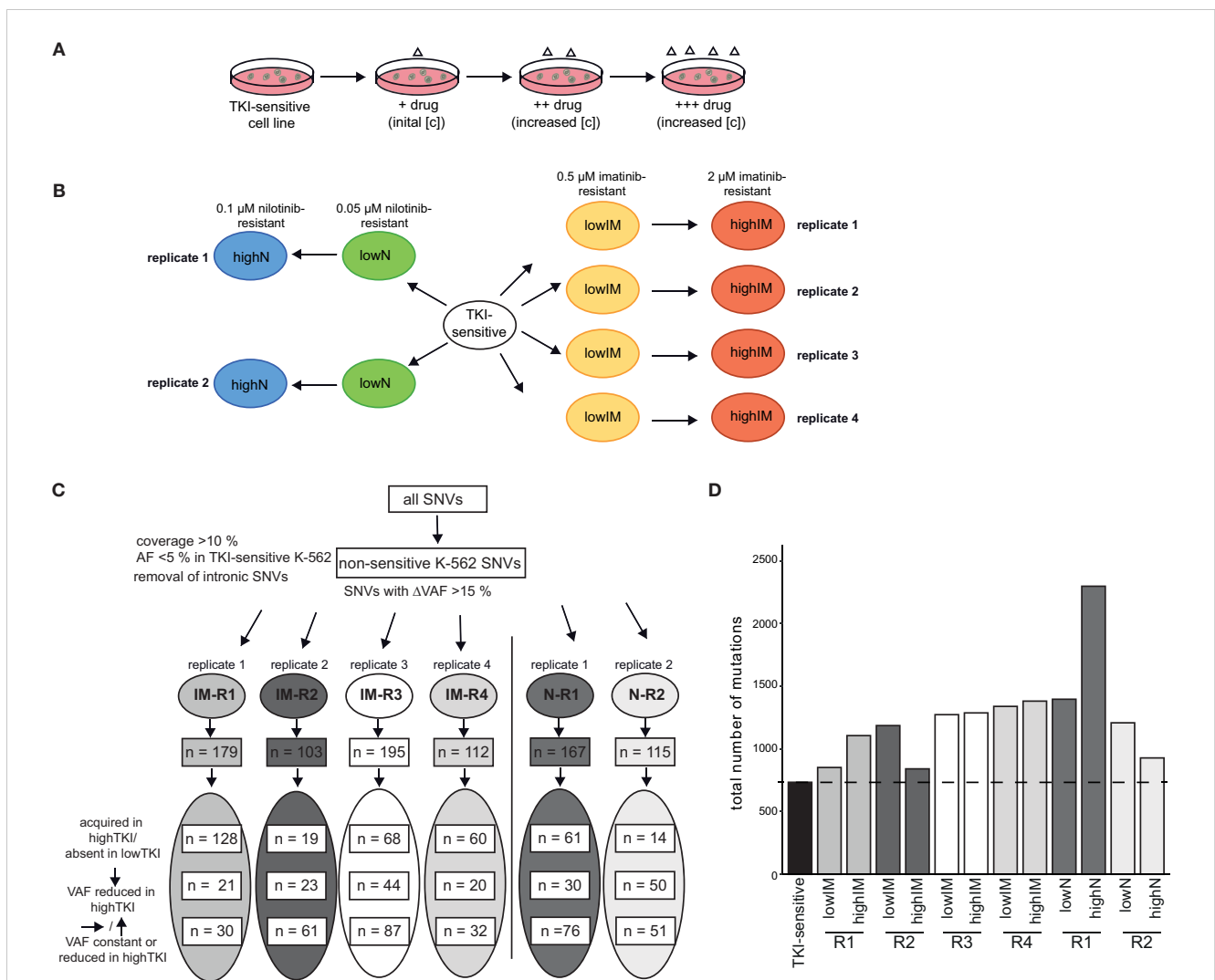


FIGURE 1

Analyses of genetic aberrations in TKI-resistant sublines. (A) Schematic representation of the generation of TKI-resistant cell lines *in vitro*. TKI-sensitive cells were exposed to an initial drug concentration (IM: 0.1 μM; N: 0.01 μM). When the cellular proliferation rate was restored, the drug concentration was stepwise increased (IM: 0.3, 0.5, 0.7, 1.0, 1.5 and 2 μM; N: 0.02, 0.05, 0.07 and 0.1 μM). (B) Overview of the TKI-resistant sublines used for the present study: Four imatinib-resistant sublines, resistant against low (0.5) and high (2 μM) imatinib, and two nilotinib-resistant sublines, resistant against low (0.05) and high (0.1 μM) nilotinib, were analyzed and compared to TKI-sensitive K-562 cells. (C) Analysis pipeline for the TKI-resistant cell lines. Using a coverage of >10%, the removal of SNVs already present in TKI-sensitive cells (VAF < 0.05) and removal of deep intronic SNVs, SNVs with a difference in the variant allele frequency (VAF) >15% between TKI-sensitive and resistant cell lines were obtained. The numbers indicate the SNVs clustered into variants acquired in highTKI/absent in lowTKI, variants with reduced VAF in highTKI and variants with constant or reduced VAF the high TKI-resistant cell lines compared to low TKI-resistant cells. (D) Total number of mutations in the TKI-resistant sublines. IM, imatinib; N, nilotinib; TKI, tyrosine kinase inhibitor; R, replicate.

(Figure 1D). However, for N-R1, a strong increase in the total SNV number was detected in highN compared to lowN, while in highIM-R2, as well as in highN-R2, the total number of SNVs was lower compared to lowIM-R2 or lowN-R2 cells, respectively (Figure 1D). To generate insight into the mutational processes, we determined the mutational signatures (COSMIC, <https://doi.org/10.11093/nar/gky1015>) of the variants that were acquired in the TKI-resistant sublines (VAF < 5% in TKI-sensitive K-562, Δ VAF > 15% between TKI-sensitive and -resistant K-562 cells). In all sublines, the signatures of unknown etiology, SBS40, showed the strongest signal (Supplementary Figure S1).

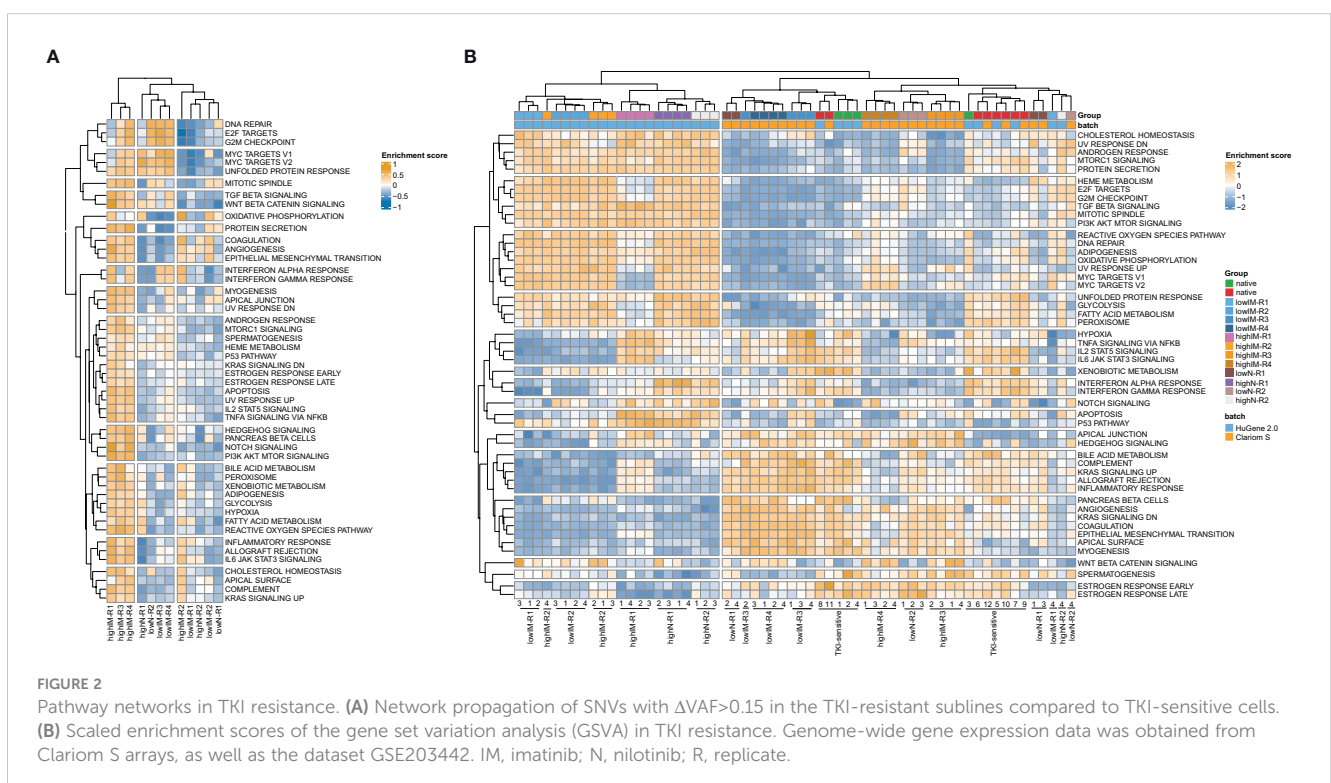
As proteins interact in protein-protein-interaction (PPI) networks, this can be analyzed using network-based approaches, such as network propagation. Following this idea, mutations in single genes (protein) can be viewed as 'heat sources' in a PPI network. This heat can diffuse through the rest of the network using an iterative process until a steady state is reached. Proteins close to the mutated protein get higher propagation scores than distant proteins following the biological assumption that proteins underlying similar phenotypes tend to interact with one another (21, 22). Accordingly, the protein-protein interaction network of acquired variants was determined.

Three clusters were revealed for the resistant cell lines and 14 clusters for gene sets with highIM-R1, -R3 and -R4 being a distinct cluster separate from the other tested resistant sublines (Figure 2A). To compare the network propagation with gene expression data, genome-wide expression analyses of the TKI-resistant cell lines and gene set variation analyses were performed [(16), Figure 2B]. The resulting pattern of enriched pathways was highly similar to one of the protein-protein interaction network derived from the mutational pattern (Figure 2A).

3.2 *In vitro*-TKI resistance is associated with pathogenic variants in well-known oncogenes

To identify potential driver mutations in the TKI-resistant sublines, acquired SNVs (with the respective AF \leq 5% in sensitive K-562 cells) were compared to a list of 568 mutational cancer driver genes previously published by Martínez-Jiménez et al. (23) (Figure 3A, Table 1). Between two and five of the detected mutations in each TKI-resistant cell line were mapped to genes from the mutational cancer driver gene list. Among the acquired variants were the well-known pathogenic RAS-family mutation *KRAS* (*KRAS* proto-oncogene, GTPase) p.(Ala59Thr) (ClinVar ID: 12581; lowIM-R3: 8.7%, highIM-R3: 66.6%) in IM-R3, *KRAS* p.(Gly12Asp) in IM-R4 (ClinVar ID: 12582; lowIM-R4: absent; highIM-R4: 29%, Figures 3A, B), as well as *NRAS* (*NRAS* proto-oncogene, GTPase) p.(Gln61Lys) (ClinVar ID: 73058; lowN: 29.2%, highN: 33.3%, Figures 3A, C) in N-R2. Further, two pathogenic *KMT2D* (lysine methyltransferase 2D) variants p.(Leu3266Val) and p.(Arg191Trp) (ClinVar ID: 449928) were acquired in IM-R3 (lowIM-R3: 9%, highIM-R3: 37%, Figures 3A, B). Moreover, *PTPN11* (protein tyrosine phosphatase non-receptor 11) p.(Tyr279Cys) was detected in IM-R2 (ClinVar ID: 13328; lowIM-R2: absent; highIM-R2: 69%, Figures 3A, B). In this cell line, the previously unknown *PDGFRB* (platelet-derived growth factor receptor beta) variant p.(Glu578Gln) was also detected (lowIM-R2: absent, highIM-R2: 28%, Figures 3A, B, Table 1). The gain of these SNVs likely explains the development of TKI resistance in the respective cell lines.

As *ABL* mutations are frequently the reason for TKI failure, mutations in this gene were also taken into focus showing two



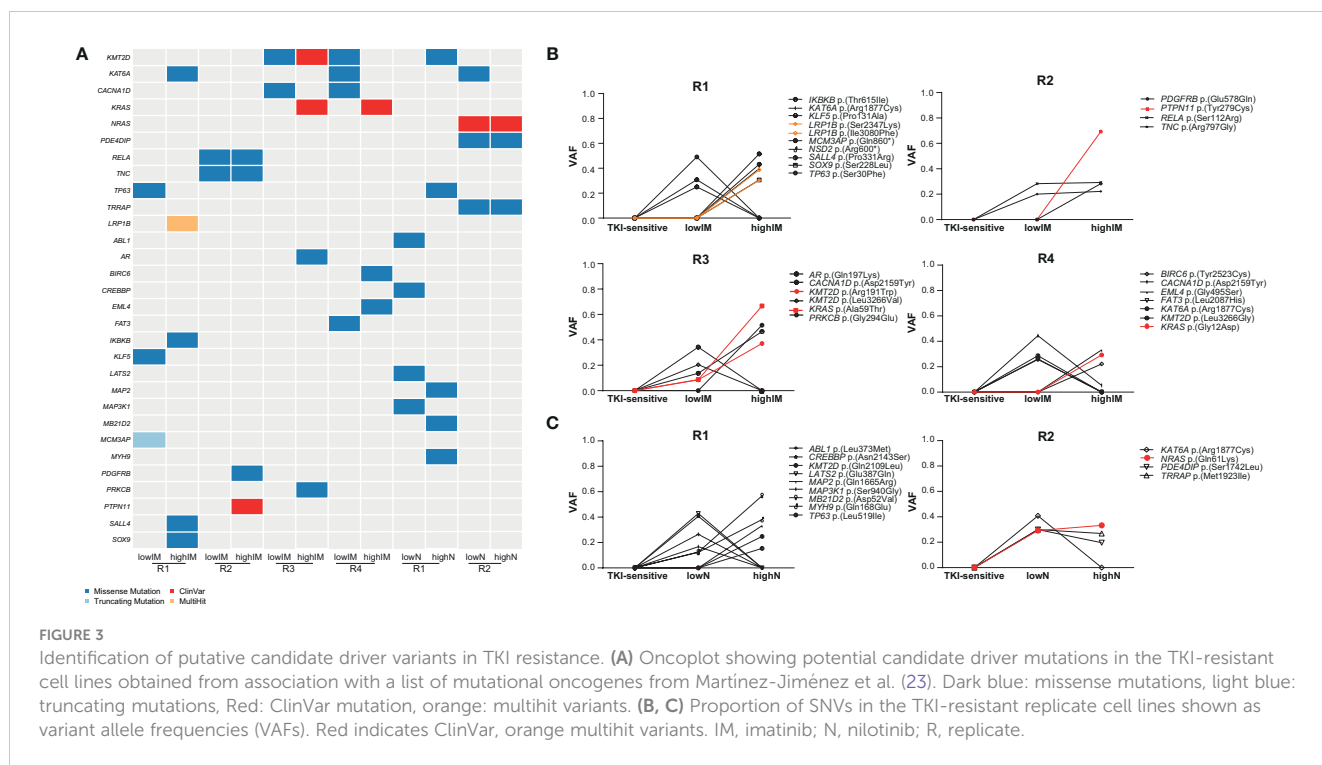


TABLE 1 Variants in tumor driver genes acquired in TKI resistance.

Gene symbol	Classification	Sample	ClinVar ID, rs-number, COSMIC ID	CADD score	VAF
ABL1	chr9: 130873012C>A NM_007313: c.1117C>A p.(Leu373Met)	lowN-R1		25.2	0.2648
AR	chrX: 67545735C>A NM_000044: c.589C>A p.(Gln197Lys)	highIM-R3		22.2	0.4655
BIRC6	chr2: 32482454A>G NM_016252: c.7568A>G p.(Tyr2523Cys)	highIM-R4		25.5	0.2222
CACNA1D	chr3: 53811368G>T NM_000720: c.6508G>T p.(Asp2170Tyr)	lowIM-R3 lowIM-R4		29	0.3429 0.4444
CREBBP	chr16: 3728619A>G NM_004380: c.6428A>G p.(Asn2143Ser)	lowN-R1	COSV52114804	10.68	0.4066
EML4	chr2: 42303119G>A NM_019063: c.1690G>A p.(Gly564Ser)	highIM-R4		32	0.3333
FAT3	chr11: 92799273T>A NM_001367949: c.6260T>A p.(Leu2087His)	lowIM-R4		26.2	0.2526
IKBKB	chr8: 42322352C>T NM_001556: c.1844C>T p.(Thr615Ile)	highIM-R1		21.1	0.5152
KAT6A	chr8: 41932591G>A NM_006766: c.5635G>A p.(Arg1879Cys)	highIM-R1 lowIM-R4 lowN-R2	rs772414652, COSV55902233	31	0.3967 0.2611 0.4081

(Continued)

TABLE 1 Continued

Gene symbol	Classification	Sample	ClinVar ID, rs-number, COSMIC ID	CADD score	VAF
KLF5	chr13: 73062263C>G NM_001730: c.664C>G p.(Pro222Ala)	lowIM-R1	COSV100890535	18.09	0.3077
KMT2D	chr12: 49041444T>A NM_003482: c.6326T>A p.(Gln2109Leu)	highN-R1		23.6	0.2481
KMT2D	chr12: 49037560G>C NM_003482: c.9796G>C p.(Leu3266Val)	lowIM-R3 lowIM-R4		23.2	0.2043 0.2875
KMT2D	chr12: 49054080G>A NM_003482: c.571G>A p.(Arg191Trp)	highIM-R3	449928, rs1555198522, COSV56467834	29.6	0.371
KRAS	chr12: 25227349C>T NM_033360: c.175C>T p.(Ala59Thr)	highIM-R3	12581, rs121913528, COSV55499283, COSV55796966	24.2	0.6667
KRAS	chr12: 25245350C>T NM_033360: c.35C>T p.(Gly12Asp)	highIM-R4	12582 rs121913529, COSV55497369 COSV55497419, COSV55497479	23.7	0.2927
LATS2	chr13: 20988621C>G NM_014572: c.1159C>G p.(Glu387Gln)	lowN-R1		17.95	0.4286
LRP1B	chr2: 140487651A>T NM_018557: c.9209A>T p.(Ile3070Lys)	highIM-R1		26.7	0.3881
LRP1B	chr2: 140598785G>A NM_018557: c.7040G>A p.(Ser2347Phe)	highIM-R1		26.6	0.304
MAP2	chr2: 209710175A>G NM_001375505: c.5483A>G p.(Glu1828Arg)	highN-R1	rs1184836325	26.1	0.3333
MAP3K1	chr5: 56882018A>G NM_005921: c.2818A>G p.(Ser940Gly)	lowN-R1		13.86	0.1667
MB21D2	chr3: 192917686T>A NM_178496: c.155T>A p.(Asp52Val)	highN-R1		28.7	0.5682
MCM3AP	chr21: 46270451G>A NM_003906: c.2578G>A p.(Gln860*)	lowIM-R1		41	0.25
MYH9	chr22: 36327477G>C NM_002473: c.502G>C p.(Gln168Glu)	highN-R1		23.9	0.381
NRAS	chr1: 114713909C>A NM_002524: c.181C>A p.(Gln61Lys)	lowN-R2 highN-R2	73058, rs121913254, COSV54736310, COSV54743343, COSV54752117	26.4	0.2917 0.3333
PDE4DIP	chr1: 149009789C>T NM_001350521: c.5333C>T p.(Ser1778Leu)	lowN-R2 highN-R2		24.1	0.3 0.1961

(Continued)

TABLE 1 Continued

Gene symbol	Classification	Sample	ClinVar ID, rs-number, COSMIC ID	CADD score	VAF
PDGFRB	chr5: 150125520G>C NM_002609: c.1732G>C p.(Glu578Gln)	highIM-R2		26.3	0.283
PRKCB	chr16: 24113032G>A NM_002738: c.881G>A p.(Gly294Glu)	highIM-R3	rs199901715	22	0.5152
PTPN11	chr12: 112473023A>G NM_01330437: c.836A>G p.(Tyr279Cys)	highIM-R2	13328, rs121918456, CM021133, CM041069, COSV61009292	29.9	0.6929
RELA	chr11: 65660125T>A NM_021975: c.426T>A p.(Gln142His)	lowIM-R2 highIM-R2		22.4	0.2828 0.2923
SALL4	chr20: 51791491G>C NM_020436: c.992G>C p.(Pro331Arg)	highIM-R1	COSV53854623	26.1	0.4322
SOX9	chr17: 72122970C>T NM_000346: c.683C>T p.(Ser228Leu)	highIM-R1	COSV55423902, COSV55424856	30	0.3066
TNC	chr9: 115081787T>C NM_002160: c.2389T>C p.(Arg797Gly)	lowIM-R2 highIM-R2		25.5	0.2 0.2222
TP63	chr3: 189737766C>T ENST00000264731: c.89C>T p.(Ser30Phe)	lowIM-R1		26.1	0.4909
TP63	chr3: 189889387C>A NM_003722: c.1555C>A p.(Leu519Ile)	highN-R1	COSV53199362, COSV99289295	21	0.1538
TRRAP	chr7: 98955211G>A NM_001375524: c.5844G>A p.(Met1948Ile)	lowN-R2 highN-R2		24.6	0.2993 0.2685

Variants in tumor driver genes according to Martínez-Jiménez et al. (22) (VAF in TKI-sensitive K-562: < 5%, Δ VAF between TKI-sensitive and -resistant K-562: >15%) including the classification, sample in which the variant was acquired, CADD score v1.6 and variant allele frequency (VAF) in the TKI-resistant sublines according to GRCh38/hg38. It should be noted that the K-562 cell line is triploid. lowIM: 0.5 μ M imatinib-resistant, highIM: 2 μ M imatinib-resistant, lowN: 0.05 μ M nilotinib-resistant, highN: 0.1 μ M nilotinib-resistant K-562 cells, R1: replicate 1, R2: replicate 2, R3: replicate 3, R4: replicate 4.

variants of unknown significance p.(Leu373Met) in lowN-R1 and p.(Glu208Asp) (VAF: 7%) in highIM-R4, as well as the known pathogenic kinase-domain mutation p.(Glu274Lys), with the latter likely associated with the TKI resistance (VAF: 10%, Figure 3A).

3.3 NRAS p.(Gln61Lys) impairs the response to TKI treatment

Presence of variants in *NRAS*, *KRAS* as well as *PTPN11*, *PDGFRB*, *RELA*, and *KMT2D* in the TKI-resistant sublines pointed to recurrent pathway changes, especially in Ras-MAP-kinase signaling (Figure 2; Figure 4A). As *NRAS* p.(Gln61Lys) is a well-known driver mutation, described in various cancer types and associated with malignancy and tumor progression, the effect of this mutation in our *in vitro*-model was analyzed to investigate whether it is solely sufficient for the development of TKI resistance and if this

effect is detectable with our *in vitro*-model (Supplementary Table S3). To address this, TKI sensitive K-562 cells were transfected with either *NRAS* wild-type or the p.(Gln61Lys) variant. The response to nilotinib was analyzed measuring cell number, metabolic rate activity, apoptosis, and proliferation rates. Successful transfection of K-562 cells led to a 4.4-fold increase in cell number after *NRAS* WT ($p < 0.001$) and 6.2-fold after p.(Gln61Lys) transfection compared to the negative control ($p < 0.001$, Figure 4B). In addition, metabolic activity was increased in *NRAS* WT (1.2-fold, $p = 0.002$) and p.(Gln61Lys)-transfected cells (5.2-fold, $p < 0.001$; Figure 4B), while apoptosis, visible on the level of caspase 9 activation, was decreased (WT: 25%; $p < 0.001$; p.(Gln61Lys): 59%, $p < 0.001$; Figure 4A). However, proliferation measured by Ki-67 expression was not significantly altered between the cell lines (Figure 4B). A similar effect was also observed under imatinib exposure, as cell number (62%, $p = 0.008$) and metabolic activity (3.7-fold, $p < 0.001$) were increased and apoptosis was reduced after

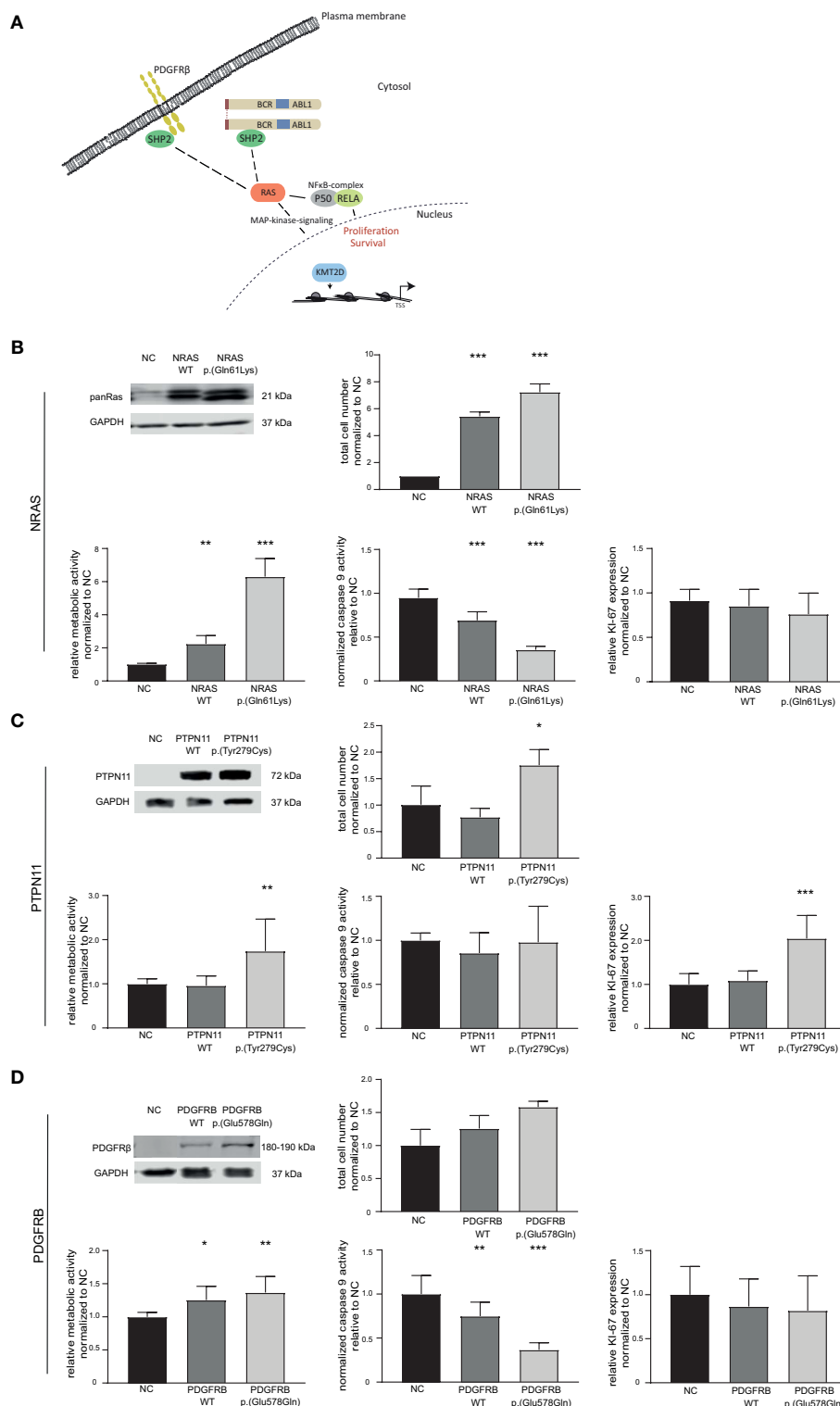


FIGURE 4

Effect of candidate variants *NRAS* p.(Gln61Lys), *PTPN11* p.(Tyr279Cys) and *PDGFRB* p.(Glu578Gln) on the response to TKI treatment. **(A)** Graphical representation of the pathways affected by variants in the candidate genes *NRAS/KRAS*, *PTPN11* (encoding SHP2), *PDGFRB* and *KMT2D*. **(B–D)** Top left: Western Blot of successful transfection of wild-type (WT) and variant into TKI-sensitive K-562 cells compared to GAPDH. Cellular fitness after WT and variant transfection and 48 h nilotinib exposure (0.1 μ M) for **(B)** *NRAS* WT and p.(Gln61Lys), as well as imatinib exposure (2 μ M) for **(C)** *PTPN11* WT and p.(Tyr279Cys) and **(D)** *PDGFRB* WT and p.(Glu578Gln). Top right: Total cell number analyzed using trypan blue staining. Bottom left: Metabolic activity measured by WST assay. Bottom middle: Caspase 9 activity analyzed by caspase 9-Glo assay. Bottom right: Ki-67 expression to investigate cellular proliferation. Data was normalized to respective negative control (NC) and analyzed using Two-way ANOVA followed by Dunnett's test. N = 3. Error bars indicate standard deviation. * $p < 0.05$, ** $p < 0.01$, *** $p < 0.001$.

NRAS p.(Gln61Lys) transfection (-45%, $p = 0.003$), while proliferation did not significantly change (Supplementary Figure S2). Overall, our data demonstrate that the presence of *NRAS* p.(Gln61Lys) is solely sufficient to promote TKI resistance.

3.4 *PTPN11* p.(Tyr279Cys), but not *PDGFRB* p.(Glu578Gln) promote the development of imatinib resistance

Using our established *in vitro*-analysis pipeline, we focused on the *PTPN11* p.(Tyr279Cys) variant (IM-R2: VAF: 48%, Supplementary Table S3). Successful transfection of *PTPN11* p.(Tyr279Cys) into sensitive K-562 cells led to an increase in cell number (1.7-fold, $p = 0.03$), accompanied by an increase in metabolic activity (1.7-fold, $p = 0.005$) and proliferation (2.0-fold, $p < 0.001$). Nevertheless, a change in apoptosis was not observed (Figure 4C).

PTPN11 p.(Tyr279Cys) is a well-known pathogenic germline variant associated with Leopard- and Noonan-syndrome (24, 25). However, this particular variant's role in cancer and CML is widely unknown. To investigate the effect of *PTPN11* p.(Tyr279Cys) in imatinib resistance and on the context-dependent protein function, first, *PTPN11* expression was analyzed in the imatinib-resistant sublines showing no expression differences compared to TKI-sensitive K-562 cells (Supplementary Figure S3). As several studies indicated a loss of catalytic function for *PTPN11* p.(Tyr279Cys) (26), we hypothesized that the observed effect could be due to altered phosphatase activity. To address this, TKI-sensitive K-562 cells were exposed to the *PTPN11* inhibitor RMC-4450, and the effects on Ras-MAP-kinase signaling were analyzed on the level of ERK activation. As expected, *PTPN11* inhibition reduced the phosphorylation of ERK (Supplementary Figure S4A). To investigate if *PTPN11* blockade alters the response to imatinib, an siRNA-mediated knockdown of *PTPN11* was performed to mimic reduced protein levels (Supplementary Figure S4B). The knockdown cells were subsequently exposed to imatinib resulting in decreased metabolic activity (-32%, $p < 0.001$) and BrdU incorporation (-33%, $p = 0.02$), while apoptosis was not altered (Supplementary Figure S4C). Moreover, *PTPN11* inhibition was performed in the imatinib-resistant cell lines to investigate the extent of pathway addiction in these cells. Interestingly, *PTPN11* inhibition only resulted in reduced ERK-phosphorylation in highIM-R2 (-1.3-fold, $p = 0.04$), but not in the other resistant sublines (Supplementary Figure S4D). The siRNA-mediated knockdown of *PTPN11* in this cell line showed a slight decrease in imatinib susceptibility, as BrdU incorporation was 1.3-fold increased ($p = 0.02$), while metabolic activity and apoptosis were not altered (Supplementary Figures S4E, F).

As a further candidate variant, we analyzed *PDGFRB* p.(Glu578Gln), as *PDGFRB* is a well-known target of imatinib (IM-R2: VAF: 34%, Supplementary Table S3). Although overexpression of *PDGFRB* p.(Glu578Gln) did not lead to a significant increase in cell number, metabolic activity was increased (WT: 1.3-fold, $p = 0.01$; p.(Glu578Gln): 1.4-fold, $p = 0.002$) and caspase 9 activity reduced after WT and p.(Glu578Gln)

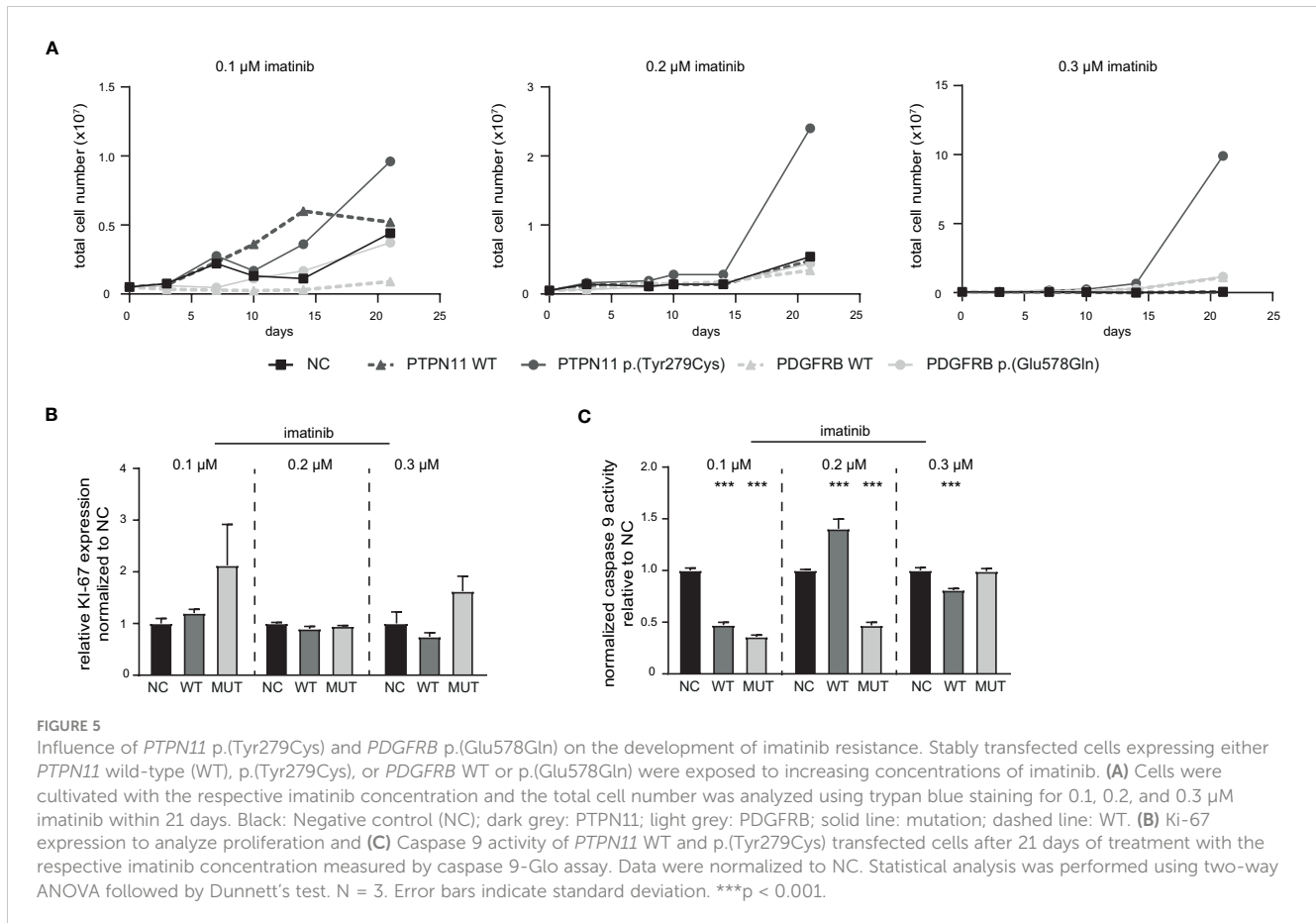
transfection (WT: 25%, $p = 0.007$; p.(Glu578Gln): 74%, $p < 0.001$). Analyses of proliferation measured by Ki-67 expression did not reveal significant differences (Figure 4D).

Next, stably transfected cell lines expressing either *PTPN11* WT or p.(Tyr279Cys), as well as *PDGFRB* WT or p.(Glu578Gln) were generated. These cell lines were exposed to low dose imatinib (0.1 to 0.3 μM) and the total cell number was analyzed during the development of imatinib resistance in a time-frame of 21 days (Figure 5). An increase in the cell number of *PTPN11* p.(Tyr279Cys)-expressing cells were detected in all tested imatinib concentrations, while the other cell lines showed no differences compared to the negative control-transfected cells (Figure 5A). As *PTPN11* p.(Tyr279Cys) seemed to promote an advantage for the cells during the development of imatinib resistance, proliferation and apoptosis in these cell lines after two weeks of exposure to the respective imatinib concentration was analyzed. Compared to WT and negative control-transfected cells, no significant increase in the proliferation of p.(Y279)-transfected cells was detected (Figure 5B). An imatinib dose-dependent effect was observed in WT-expressing cells on apoptosis (0.1 μM : -53%, $p < 0.001$; 0.2 μM : +40%, $p < 0.001$; 0.3 μM : -19%, $p < 0.001$), while cells harboring p.(Tyr279Cys) showed reduced apoptosis in 0.1 μM (74%, $p < 0.001$) and 0.2 μM imatinib-resistant cells (53%, $p < 0.001$), but not in resistance to 0.3 μM imatinib (Figure 5C).

4 Discussion

Tumor cells undergoing anti-cancer therapy underlie clonal evolution and selection, a major obstacle to successful treatment. In chronic myeloid leukemia, 20-25% of patients suffer from therapy failure within 5 years of TKI treatment (5). In half of the patients, mutations in the BCR::ABL1 kinase are detected, resulting in loss of TKI binding and, subsequently, resistance (4). For the other half of the patients, the resistance mechanisms are unknown. To generate insights into mechanisms of TKI resistance, an *in vitro*-TKI resistance model derived from TKI-sensitive K-562 CML cells during long-term drug exposure was established. For this purpose, biological replicates of imatinib and nilotinib resistance were generated obtaining sublines resistant against 0.5 and 2 μM imatinib, and 0.05 and 0.1 μM nilotinib, respectively. In CML patients, the imatinib plasma levels varied between 0.34 and 3.4 μM (27, 28). Thus, the imatinib concentrations of 0.5 and 2 μM were used to reflect the fluctuations. As nilotinib is known to have a 20-fold higher potency than imatinib (6), cells resistant to a maximum of 0.1 μM were used for the present study.

Large differences between the sublines were observed analyzing the mutational landscape of the TKI-resistant cell lines. The two cell lines harboring variants in the oncogene *KRAS* (highIM-R3, highIM-R4), showed a high similarity in the protein-protein interaction network compared to TKI-sensitive K-562 cells. These are likely to be addressed by the overall gained variants and are also visible in the gene expression profiles. Although the number of variants gradually increased during the development of imatinib resistance in both cell lines, in IM-R3 *KRAS* p.(Ala59Thr)



accompanied by *KMT2D* p.(Arg191Trp) are likely to be crucial for resistance. In IM-R4, the combination of the well-known *KRAS* p.(Gly12Asp) mutation and a low-frequency mutation in *ABL* p.(Glu274Lys) are possibly central for resistance. Consistent with these results, *RAS* mutations are known to be tumor driver variants in myeloid neoplasia and have also been identified in CML patients with therapy failure (29, 30). However, with an incidence of only 5%, mutations in *RAS* seem to be a rare event in chronic myeloid leukemia (29, 31). In general, the *KRAS*-mutated cells showed a similar network propagation cluster compared to TKI-sensitive cells pointing to restored Ras-MAP-kinase signaling being the underlying resistance mechanisms.

In N-R2, the *NRAS* p.(Gln61Lys) mutation apparently occurs early during the development of nilotinib resistance. This well-known mutation occurs in 13-25% malignant melanoma and 1-6% colorectal cancer patients, but also other tumors harbor this mutation, e.g., neuroblastoma, non-small cell lung cancer or leukemia (32). However, the pattern of *NRAS* mutations in leukemia varies widely from solid tumors with a predominance for the observed p.(Gln61) (38%) and p.(Gly12) (36%) missense mutations (29, 33). The p.(Gln61Lys) mutation leads to constitutive *NRAS* activation. It is the reason for therapy failure, as observed, e.g., for epidermal growth factor receptor (EGFR) inhibition, which makes alternative therapies necessary (34). We found that expression of *NRAS* p.(Gln61Lys) promotes survival of CML cells under TKI exposure by reduction of apoptosis and increased cell

viability, showing that this mutation is likely the main cause of resistance of our nilotinib-resistant subline N-R2. As *NRAS* p.(Gln61Lys) is already present in lowN and provides a strong benefit for the clones harboring this mutation, this indicates clonal selection and might also be a reason for the quite low overall number of mutations in this resistant subline compared to the other cell lines. Overall, these findings show that our *in vitro*-CML drug resistance model is suitable for detecting genetic aberrations promoting TKI resistance, among them pathogenic variants that have already been detected in other tumor entities. Therefore, we used the established analysis pipeline to investigate further candidate mutations.

Similar to N-R2, the overall number of acquired variants was quite low for IM-R2. Although the *PTPN11* p.(Tyr279Cys) and *PDGFRB* p.(Glu578Gln) variants were acquired in the late development of TKI resistance in highIM-R2, the allele frequencies were high in this cell line. This indicates a benefit for the clones harboring these variants. *PTPN11*/*SH2P2* is a non-receptor phosphatase involved in fine-tuning of cell signaling by binding to its adaptor proteins Grb2 and Gab1 and is considered a positive regulator of *RAS* signaling (35). *PTPN11* germline variants are present in 50% of patients suffering from Noonan-syndrome, an autosomal dominant disorder associated with heart failure and facial dysmorphism (25), or Leopard syndrome, a genetic disease mainly leading to heart and skin anomalies (24). In about 85% of patients, missense variants in *PTPN11* are observed, including the

variant p.(Tyr279Cys), as detected in the present study. Further, somatic *PTPN11* variants occur in 34% of juvenile myelomonocytic leukemia and were also detected in other myelodysplastic syndromes, yet to a smaller extent (36). The main observed variants in *PTPN11* affect residues in the N-terminal Src homology (N-SH2) or the protein tyrosine phosphatase (PTP) domain interacting surface and likely result in a gain of function. This led to the description of *PTPN11* as an atypical phosphatase with oncogenic properties, which makes *PTPN11* a suitable target for cancer therapy (36, 37). It was shown that inhibition of *PTPN11* might be an effective strategy to overcome *NRAS*-dependent resistance in neuroblastoma or *KIT*-induced myeloproliferative diseases (38, 39).

In the present study, a decreased imatinib response in the presence of *PTPN11* p.(Tyr279Cys) was observed with increased proliferation rates. In CML, *PTPN11* variant (NM_002834.5:c.1529A>T) p.(Gln510Leu), which is also a known variant in Noonan-syndrome (RCV001261023.1), was detected in a patient suffering from blast crisis after 10 years of TKI treatment (40). Further, it was demonstrated that *PTPN11* is necessary for *BCR::ABL1*-induced hematologic neoplasms, as its deletion compromised induction of CML in mice (41). In a study in K-562 cells, it was shown that *PTPN11* phosphorylation is induced during imatinib exposure as well as resistance and *PTPN11* inhibition is able to restore TKI response (42). However, for p.(Tyr279Cys) in Leopard syndrome, a loss of catalytic activity was demonstrated (26, 43). It is likely that the observed variant in *PTPN11* results in an alteration of the phosphatase activity, which contributes to the development of TKI resistance. Nevertheless, further studies are necessary to investigate the effect of *PTPN11* p.(Tyr279Cys) in more detail. The relevance of *PTPN11* in CML is also stressed by findings on CD34+ CML stem cells harboring the pathogenic *PTPN11* p.(Gly60Val) resulting in sustained Ras-MAP-signaling pathway activation. Interestingly, the resistance in these cells could be overcome by synergistic usage of TKIs and integrated stress response inhibitors that prevent the cellular response to the external and internal stress stimuli, such as imatinib (44). This could be a very promising approach in TKI-resistant CML patients.

We detected the *PDGFRB* p.(Glu578Gln) variant in the same imatinib-resistant subline. This tyrosine kinase is a known target of imatinib and is implicated in multiple diseases, e.g., dermatofibrosarcoma protuberans or myofibromatosis (45). Several variants, but also genetic rearrangements, in *PDGFRB* were shown to be associated with TKI resistance (46). The observed p.(Glu578Gln) variant is located in the juxtamembrane portion of the protein and has not been described yet. Interestingly, it was shown that *PTPN11* can suppress transformation induced by *PDGFRB*, suggesting a strong link between these two proteins (47). Therefore, it can be hypothesized that the two variants in *PDGFRB* and *PTPN11* can circumvent imatinib-induced *BCR::ABL1* inhibition and contribute to the manifestation of TKI resistance. Thus, monitoring of variants in these genes should be performed in TKI-relapsed CML patients.

For IM-R1 and N-R1, no clear candidate driver variants were observed. Moreover, these cells clustered apart from the other cell lines in the network propagation. Potentially, the clones have a

diverse mechanism of resistance which is reflected by a diverse pattern of variants. As previously mentioned, CML resistance occurs either due to *BCR::ABL1*-dependent or -independent mechanisms. It is widely known that especially mutations in *BCR::ABL1* affect TKI-response and lead to relapse due to the uprising of mutated clones (48). Beyond *BCR::ABL1*, variants in the epigenetic modulator DNA (cytosine-5)-methyltransferase 3A (*DNMT3A*), the polycomb group protein additional sex comb-like 1 (*ASXL1*), runt-related transcription factor 1 (*RUNX1*) and Tet methylcytosine dioxygenase 2 (*TET2*) were shown to be associated with therapy failure indicating defective epigenetic DNA regulation in TKI-resistant CML as already described for other myeloproliferative syndromes (12, 49–51). In the present study, we did not detect variants in these genes but identified several putative candidate genes that likely contribute to TKI resistance. With *NRAS*, *KRAS*, *PTPN11*, and *KMT2D*, we detected variants in genes that were shown to be mutated in low frequencies in blast crisis, but to a lower extent also in chronic phase CML (52). These findings suggest an NGS-based screening of TKI-resistant patients without *BCR::ABL1* mutations to identify potential variants responsible for therapy failure. Either detected variants or the altered downstream pathways could be future therapeutic options to be targeted by synergistic approaches to overcome TKI resistance.

In conclusion, the TKI-resistant sublines newly acquired candidate driver mutations, especially the well-known *NRAS* p.(Gln61Lys), *KRAS* p.(Ala59Thr) and p.(Gly12Asp), but also *PTPN11* p.(Tyr279Cys) affected the same signaling pathway. The gain of these variants likely explains the main mechanism resistance in the respective cell lines. It shows that such models are potentially useful to get insight into mechanisms of drug resistance and to find novel tumor driver genes or novel driver mutations. This knowledge can be used to better interpret TKI resistance in patients and, vice versa, our *in vitro*-model can be used to analyze and assess mutations observed in resistant patients. This strategy can open new options for the development of new therapy strategies.

Data availability statement

The datasets presented in this study can be found in online repositories. The whole exome sequencing data of TKI-resistant cell lines have been submitted to the European Nucleotide Archive (ENA) and is publicly available under accession number PRJEB60565. Genome-wide expression datasets are available in the GEO repository GSE227347.

Author contributions

MK and IN conceptualized the study and designed the research. PO and SV performed the experiments. AK, DE, MM, IV, MK, and IN analyzed the data. MK and IN interpreted the data. HB, MS and IC provided methodology. MK and IN wrote the original draft. All authors read and approved the final version of the manuscript.

Funding

This study was funded by a grant from the Medical Faculty of the University of Kiel. HB acknowledges funding by the Deutsche Forschungsgemeinschaft (DFG, German Research Foundation) under Germany's Excellence Strategy – EXC22167-390884018.

Acknowledgments

We thank Irina Naujoks, Anna Jürgensen and Britta Schwarten for outstanding technical assistance. We thank the Institute of Clinical Molecular Biology in Kiel for providing Sanger sequencing, as partly supported by the DFG Clusters of Excellence “Precision Medicine in Chronic Inflammation” and “ROOTS”. We thank Claudia Becher from the Institute of Human Genetics in Kiel for her technical assistance. AK thanks the computational support from the OMICS compute cluster at the University of Lübeck.

References

- Luchini C, Lawlor RT, Milella M, Scarpa A. Molecular tumor boards in clinical practice. *Trends Cancer* (2020) 6:738–44. doi: 10.1016/j.trecan.2020.05.008
- Deininger MW, Goldman JM, Melo JV. The molecular biology of chronic myeloid leukemia. *Blood* (2000) 96:3343–56. doi: 10.1182/blood.V96.10.3343
- Druker BJ, Guilhot F, O'Brien SG, Gathmann I, Kantarjian H, Gattermann N, et al. Five-year follow-up of patients receiving imatinib for chronic myeloid leukemia. *N Engl J Med* (2006) 355:2408–17. doi: 10.1056/NEJMoa062867
- Milojkovic D, Apperley J. Mechanisms of resistance to imatinib and second-generation tyrosine inhibitors in chronic myeloid leukemia. *Clin Cancer Res* (2009) 15:7519–27. doi: 10.1158/1078-0432.CCR-09-1068
- Hochhaus A, Larson RA, Guilhot F, Radich JP, Branford S, Hughes TP, et al. Long-term outcomes of imatinib treatment for chronic myeloid leukemia. *N Engl J Med* (2017) 376:917–27. doi: 10.1056/NEJMoa1609324
- Baccarani M, Deininger MW, Rosti G, Hochhaus A, Soverini S, Apperley JF, et al. European LeukemiaNet recommendations for the management of chronic myeloid leukemia: 2013. *Blood* (2013) 122:872–84. doi: 10.1182/blood-2013-05-501569
- Soverini S, De Benedittis C, Papayannidis C, Paolini S, Venturi C, Iacobucci I, et al. Drug resistance and BCR-ABL kinase domain mutations in Philadelphia chromosome-positive acute lymphoblastic leukemia from the imatinib to the second-generation tyrosine kinase inhibitor era: the main changes are in the type of mutations, but not in the frequency of mutation involvement. *Cancer* (2014) 120:1002–9. doi: 10.1002/cncr.28522
- Zabriskie MS, Eide CA, Tantravahi SK, Vellore NA, Estrada J, Nicolini FE, et al. BCR-ABL1 compound mutations combining key kinase domain positions confer clinical resistance to ponatinib in ph chromosome-positive leukemia. *Cancer Cell* (2014) 26:428–42. doi: 10.1016/j.ccr.2014.07.006
- Bixby D, Talpaz M. Seeking the causes and solutions to imatinib-resistance in chronic myeloid leukemia. *Leukemia* (2011) 25:7–22. doi: 10.1038/leu.2010.238
- Kaehler M, Cascorbi I. Pharmacogenomics of impaired tyrosine kinase inhibitor response: lessons learned from chronic myelogenous leukemia. *Front Pharmacol* (2021) 12:696960. doi: 10.3389/fphar.2021.696960
- Eiring AM, Deininger MW. Individualizing kinase-targeted cancer therapy: the paradigm of chronic myeloid leukemia. *Genome Biol* (2014) 15:461. doi: 10.1186/s13059-014-0461-8
- Schmidt M, Rinke J, Schafer V, Schnittger S, Kohlmann A, Obstfelder E, et al. Molecular-defined clonal evolution in patients with chronic myeloid leukemia independent of the BCR-ABL status. *Leukemia* (2014) 28:2292–9. doi: 10.1038/leu.2014.272
- Mirabelli P, Coppola L, Salvatore M. Cancer cell lines are useful model systems for medical research. *Cancers (Basel)* (2019) 11:1098. doi: 10.3390/cancers11081098
- Lozzio CB, Lozzio BB. Human chronic myelogenous leukemia cell-line with positive Philadelphia chromosome. *Blood* (1975) 45:321–34. doi: 10.1182/blood.V45.3.321.321

Conflict of interest

The authors declare that the research was conducted in the absence of any commercial or financial relationships that could be construed as a potential conflict of interest.

Publisher's note

All claims expressed in this article are solely those of the authors and do not necessarily represent those of their affiliated organizations, or those of the publisher, the editors and the reviewers. Any product that may be evaluated in this article, or claim that may be made by its manufacturer, is not guaranteed or endorsed by the publisher.

Supplementary material

The Supplementary Material for this article can be found online at: <https://www.frontiersin.org/articles/10.3389/fonc.2023.1200897/full#supplementary-material>

- Turrini E, Haenisch S, Laechelt S, Diewock T, Bruhn O, Cascorbi I. MicroRNA profiling in K-562 cells under imatinib treatment: influence of miR-212 and miR-328 on ABCG2 expression. *Pharmacogenet Genomics* (2012) 22:198–205. doi: 10.1097/FPC.0b013e328350012b
- Kaehler M, Litterst M, Kolarova J, Bohm R, Bruckmueller H, Ammerpohl O, et al. Genome-wide expression and methylation analyses reveal aberrant cell adhesion signaling in tyrosine kinase inhibitor-resistant CML cells. *Oncol Rep* (2022) 48:144. doi: 10.3892/or.2022.8355
- Kunstner A, Schwarting J, Witte HM, Bernard V, Stolting S, Kusch K, et al. Integrative molecular profiling identifies two molecularly and clinically distinct subtypes of blastic plasmacytoid dendritic cell neoplasm. *Blood Cancer J* (2022) 12:101. doi: 10.1038/s41408-022-00699-1
- Kaehler M, Dworschak M, Rodin JP, Ruemenapp J, Vater I, Penas EMM, et al. Zfp361 plays an ambiguous role in the regulation of cell expansion and negatively regulates Cdkn1a in chronic myeloid leukemia cells. *Exp Hematol* (2021) 99:54–64. doi: 10.1016/j.exphem.2021.05.006
- Kaehler M, Ruemenapp J, Gonnermann D, Nagel I, Bruhn O, Haenisch S, et al. MicroRNA-212/ABCG2-axis contributes to development of imatinib-resistance in leukemic cells. *Oncotarget* (2017) 8:92018–31. doi: 10.18632/oncotarget.21272
- Waetzig V, Haeusgen W, Andres C, Frehse S, Reinecke K, Bruckmueller H, et al. Retinoic acid-induced survival effects in SH-SY5Y neuroblastoma cells. *J Cell Biochem* (2019) 120:5974–86. doi: 10.1002/jcb.27885
- Menche J, Sharma A, Kitsak M, Ghiassian SD, Vidal M, Loscalzo J, et al. Disease networks. uncovering disease-disease relationships through the incomplete interactome. *Science* (2015) 347:1257601. doi: 10.1126/science.1257601
- Cowen L, Ideker T, Raphael BJ, Sharan R. Network propagation: a universal amplifier of genetic associations. *Nat Rev Genet* (2017) 18:551–62. doi: 10.1038/nrg.2017.38
- Martinez-Jimenez F, Muinos F, Sentis I, Deu-Pons J, Reyes-Salazar I, Arnedo-Pac C, et al. A compendium of mutational cancer driver genes. *Nat Rev Cancer* (2020) 20:555–72. doi: 10.1038/s41568-020-0290-x
- Sarkozy A, Digilio MC, Dallapiccola B. Leopard syndrome. *Orphanet J Rare Dis* (2008) 3:13. doi: 10.1186/1750-1172-3-13
- El Bouchikhi I, Belhassan K, Moufid FZ, Iraqui Houssaini M, Bouguenouch L, Samri I, et al. Noonan syndrome-causing genes: molecular update and an assessment of the mutation rate. *Int J Pediatr Adolesc Med* (2016) 3:133–42. doi: 10.1016/j.jipam.2016.06.003
- Tartaglia M, Martinelli S, Stella L, Bocchinfuso G, Flex E, Cordeddu V, et al. Diversity and functional consequences of germline and somatic PTPN11 mutations in human disease. *Am J Hum Genet* (2006) 78:279–90. doi: 10.1086/499925
- Leveque D, Maloisel F. Clinical pharmacokinetics of imatinib mesylate. *In Vivo (Athens Greece)* (2005) 19:77–84. doi: 10.2165/00003088-200544090-00001

28. Picard S, Titier K, Etienne G, Teilhet E, Ducint D, Bernard MA, et al. Trough imatinib plasma levels are associated with both cytogenetic and molecular responses to standard-dose imatinib in chronic myeloid leukemia. *Blood* (2007) 109:3496–9. doi: 10.1182/blood-2006-07-036012
29. Fernandez-Medarde A, Santos E. Ras in cancer and developmental diseases. *Genes Cancer* (2011) 2:344–58. doi: 10.1177/1947601911411084
30. Waanders E, Gu Z, Dobson SM, Antic Z, Crawford JC, Ma X, et al. Mutational landscape and patterns of clonal evolution in relapsed pediatric acute lymphoblastic leukemia. *Blood Cancer Discovery* (2020) 1:96–111. doi: 10.1158/0008-5472.BCD-19-0041
31. Ouerhani S, Bougateg K, Soltani I, Elgaaied AB, Abbas S, Menif S. The prevalence and prognostic significance of KRAS mutation in bladder cancer, chronic myeloid leukemia and colorectal cancer. *Mol Biol Rep* (2013) 40:4109–14. doi: 10.1007/s11033-013-2512-8
32. De Roock W, De Vriendt V, Normanno N, Ciardiello F, Tejpar S. KRAS, BRAF, PIK3CA, and PTEN mutations: implications for targeted therapies in metastatic colorectal cancer. *Lancet Oncol* (2011) 12:594–603. doi: 10.1016/S1470-2045(10)70209-6
33. Munoz-Maldonado C, Zimmer Y, Medova M. A comparative analysis of individual RAS mutations in cancer biology. *Front Oncol* (2019) 9:1088. doi: 10.3389/fonc.2019.01088
34. De Roock W, Claes B, Bernasconi D, De Schutter J, Biesmans B, Fountzilias G, et al. Effects of KRAS, BRAF, NRAS, and PIK3CA mutations on the efficacy of cetuximab plus chemotherapy in chemotherapy-refractory metastatic colorectal cancer: a retrospective consortium analysis. *Lancet Oncol* (2010) 11:753–62. doi: 10.1016/S1470-2045(10)70130-3
35. Shi ZQ, Yu DH, Park M, Marshall M, Feng GS. Molecular mechanism for the shp-2 tyrosine phosphatase function in promoting growth factor stimulation of erk activity. *Mol Cell Biol* (2000) 20:1526–36. doi: 10.1128/MCB.20.5.1526-1536.2000
36. Tartaglia M, Niemeyer CM, Fragale A, Song X, Buechner J, Jung A, et al. Somatic mutations in PTPN11 in juvenile myelomonocytic leukemia, myelodysplastic syndromes and acute myeloid leukemia. *Nat Genet* (2003) 34:148–50. doi: 10.1038/ng1156
37. Liu Q, Qu J, Zhao M, Xu Q, Sun Y. Targeting SHP2 as a promising strategy for cancer immunotherapy. *Pharmacol Res* (2020) 152:104595. doi: 10.1016/j.phrs.2019.104595
38. Mali RS, Ma P, Zeng LF, Martin H, Ramdas B, He Y, et al. Role of SHP2 phosphatase in KIT-induced transformation: identification of SHP2 as a druggable target in diseases involving oncogenic KIT. *Blood* (2012) 120:2669–78. doi: 10.1182/blood-2011-08-375873
39. Valencia-Sama I, Ladumor Y, Kee L, Adderley T, Christopher G, Robinson CM, et al. NRAS status determines sensitivity to SHP2 inhibitor combination therapies targeting the RAS-MAPK pathway in neuroblastoma. *Cancer Res* (2020) 80:3413–23. doi: 10.1158/0008-5472.CAN-19-3822
40. Sklarz LM, Wittke C, Krohn S, GROßE-Thie C, Junghans C, Murua Escobar H, et al. Genetic mutations in a patient with chronic myeloid leukemia showing blast crisis 10 years after presentation. *Anticancer Res* (2018) 38:3961–6. doi: 10.21873/anticancer.12682
41. Gu S, Sayad A, Chan G, Yang W, Lu Z, Virtanen C, et al. SHP2 is required for BCR-ABL1-induced hematologic neoplasia. *Leukemia* (2018) 32:203–13. doi: 10.1038/leu.2017.250
42. Li X, Pang J, Xue W, Wang Y, Tian T, Elgehama A, et al. Inducible SHP-2 activation confers resistance to imatinib in drug-tolerant chronic myeloid leukemia cells. *Toxicol Appl Pharmacol* (2018) 360:249–56. doi: 10.1016/j.taap.2018.09.044
43. Liu WS, Wang RR, Li WY, Rong M, Liu CL, Ma Y, et al. Investigating the reason for loss-of-function of src homology 2 domain-containing protein tyrosine phosphatase 2 (SHP2) caused by Y279C mutation through molecular dynamics simulation. *J Biomol Struct Dyn* (2020) 38:2509–20. doi: 10.1080/07391102.2019.1634641
44. Dudka W, Hoser G, Mondal SS, Tuross-Korgul L, Swatler J, Kusio-Kobialka M, et al. Targeting integrated stress response with ISRIB combined with imatinib treatment attenuates RAS/RAF/MAPK and STAT5 signaling and eradicates chronic myeloid leukemia cells. *BMC Cancer* (2022) 22:1254. doi: 10.1186/s12885-022-10289-w
45. Moura D, De Oliveira JRM. The master of puppets: pleiotropy of PDGFRB and its relationship to multiple diseases. *J Mol Neurosci* (2020) 70:2102–6. doi: 10.1007/s12031-020-01618-4
46. Bastie JN, Garcia I, Terre C, Cross NC, Mahon FX, Castaigne S. Lack of response to imatinib mesylate in a patient with accelerated phase myeloproliferative disorder with rearrangement of the platelet-derived growth factor receptor beta-gene. *Haematologica* (2004) 89:1263–4.
47. Jazayeri A, Mcgee J, Shimamura T, Cross SB, Bejcek BE. SHP-2 can suppress transformation induced by platelet-derived growth factor. *Exp Cell Res* (2000) 254:197–203. doi: 10.1006/excr.1999.4741
48. Von Bubnoff N, Schneller F, Peschel C, Duyster J. BCR-ABL gene mutations in relation to clinical resistance of Philadelphia-chromosome-positive leukaemia to STI571: a prospective study. *Lancet* (2002) 359:487–91. doi: 10.1016/S0140-6736(02)07679-1
49. Delhommeau F, Dupont S, Della Valle V, James C, Trannoy S, Masse A, et al. Mutation in TET2 in myeloid cancers. *N Engl J Med* (2009) 360:2289–301. doi: 10.1056/NEJMoa0810069
50. Asada S, Fujino T, Goyama S, Kitamura T. The role of ASXL1 in hematopoiesis and myeloid malignancies. *Cell Mol Life Sci* (2019) 76:2511–23. doi: 10.1007/s00018-019-03084-7
51. Ochi Y, Yoshida K, Huang YJ, Kuo MC, Nannya Y, Sasaki K, et al. Clonal evolution and clinical implications of genetic abnormalities in blastic transformation of chronic myeloid leukaemia. *Nat Commun* (2021) 12:2833. doi: 10.1038/s41467-021-23097-w
52. Adnan-Awad S, Kankainen M, Mustjoki S. Mutational landscape of chronic myeloid leukemia: more than a single oncogene leukemia. *Leuk Lymphoma* (2021) 62:2064–78. doi: 10.1080/10428194.2021.1894652